EUROPEAN JOURNAL OF ENTOMOLOGY
ISSN (online): 1802-8829
http://www.eje.cz
Eur. J. Entomol. **123**: 136–147, 2026
doi: 10.14411/eje.2026.014
ORIGINAL ARTICLE

Invasive risk of *Solenopsis invicta* (Hymenoptera: Formicidae) in China under current and future climate change scenarios

HAROON[1,*,**], **RIAZ HUSSAIN**[2,*], **CAI WANG**[1] and **SHENGNAN ZHANG**[3,**]

[1] College of Forestry and Landscape Architecture, South China Agricultural University, Guangzhou 510642, P.R. China; e-mails: haroon@scau.edu.cn, wangcai@scau.edu.cn

[2] College of Life Sciences, Northwest University, Xi'an 710069, P.R. China; e-mail: riazzoo123456@gmail.com

[3] Anhui Province Laboratory of Microbial Control, School of Forestry & Landscape Architecture, Anhui Agricultural University, Hefei 230036, P.R. China; e-mail: shengnan@ahau.edu.cn

Key words. Red imported fire ant, MaxEnt model, distribution pattern, risk areas, management

Abstract. The red imported fire ant (*Solenopsis invicta* Buren, 1972), is native to tropical and subtropical South America but has become a highly invasive species in parts of the southern United States, the Caribbean, and southern China. RIFA has caused significant ecological disruption through rapid colonization and aggressive behavior, affecting ecosystems and human health. This study aimed to examine the impact of different variables on the distribution of *S. invicta* throughout China and to predict its risk areas under the Current (1970–2000) and future climate change scenarios (2070s) using the ACCESS1-0 and BCC-CSM1-1 climate models. According to the MaxEnt model, under current climatic conditions, the total risk area of *S. invicta* was 2.554 million km^2, covering 27.52% of the study area. In the 2070s, high-risk areas are projected to increase by 1.72-fold and 1.68-fold under ACCESS1-0 and BCC-CSM1-1 scenarios, respectively. Precipitation of driest month (Bio14), mean temperature of coldest quarter (Bio11), mean temperature of warmest quarter (Bio10), pH of water, topography, mean diurnal range (Bio2), and soil organic carbon were the main factors influencing the distribution of *S. invicta*. Generalized Linear Model (GLM) was used to assess key determinants influencing *S. invicta* distribution. The GLM identified elevated land surface temperature, moderate soil moisture, organic carbon, vegetation cover, topographic diversity, and high urbanization as key factors promoting *S. invicta* proliferation, while adverse soil conditions limited suitable habitats. This research provides significant clues about the current distribution patterns of *S. invicta* and the influence of climate change, soil, physical and biological land properties, and anthropogenic activities on its distribution. Additional measures are necessary to control and prevent the continued spread of *S. invicta* in China.

1. INTRODUCTION

Red imported fire ants (RIFA) are native to South America and have become one of the most aggressive and widespread invasive ant species in many regions. Since its accidental introduction into the southern United States in the 20th century (Wojcik, 1983; Silverman & Brightwell, 2008). RIFA has spread to Australia and New Zealand (2001) (Jennings & McCubbin, 2004), including parts of Asia, such as Taiwan (2003) (Huang et al., 2004), Hong Kong (2004) (Zeng et al., 2005), and mainland China (Zhang et al., 2007), where it continues to expand its range. RIFA had infested 64,000 ha in Taiwan by 2014, thriving in diverse habitats ranging from agricultural lands to urban areas (Huang et al., 2004; Schowalter et al., 2015). RIFA belongs to the subfamily Myrmicinae and possesses a functional sting, which distinguishes it from other invasive ants, such as those in *Dolichoderinae* and *Formicinae*. It's painful, and often repeated stings can cause severe allergic reactions in humans and animals, contributing to public health concerns and reduced recreational use of infested areas. In addition to these health impacts, RIFA inflicts widespread damage on agriculture, native biodiversity, and infrastructure, resulting in substantial economic losses and ecological disruption (Siddiqui et al., 2024; Wang & Lu, 2017).

RIFA has an aggressive behavior that takes over the habitats of native ant species and expands its territory in many regions (Wojcik, 1983; Silverman & Brightwell, 2008). The global economic burden of *S. invicta* is substantial. Annual costs are estimated at US$ 70.0 billion for control and US$ 6.9 billion for health-related expenses (Wang et al., 2023; Bradshaw et al., 2016). In Hawaii, the projected annual cost is about US$ 211 million, including direct damage, control measures, and losses in recreational

* These authors contributed equally.

** Corresponding authors; e-mails: shengnan@ahau.edu.cn, haroon@scau.edu.cn

opportunities. Over the 20 years since its introduction, the cumulative economic impact in Hawaii has reached approximately US$ 2.5 billion (Gutrich et al., 2007). Across China, the annual economic impact of *S. invicta* is approximately 514 million RMB (~74.5 million USD) (Wang et al., 2023), while the cumulative control losses in Guangdong Province (2007–2020) reached 22,710.93 million RMB (~3.29 billion USD) (Li et al., 2023).

Since its first official detection in mainland China in 2004, RIFA has spread rapidly across multiple provinces (Zhang et al., 2007). Ecological modeling studies predict that the species could potentially colonize up to 25 provinces, indicating a substantial risk of further expansion (Zhang et al., 2007). Subsequent studies under different climate scenarios estimate that the potential risk area may reach approximately 8.137×10^5 km² in China (Song et al., 2021; Wang et al., 2023). These findings highlight the significant invasion potential of RIFA and the necessity of predicting its future distribution. Although extensive research has investigated the molecular identification, genetics, and biological characteristics of *S. invicta* (Morrison et al., 2004; Sung et al., 2018; Li et al., 2023), fewer studies have focused on assessing its invasion risk and potential distribution using ecological niche modeling approaches (Sutherst & Maywald, 2005; Tang et al., 2025).

Climatic suitability plays a key role in the establishment and invasion of new areas for invasive species, such as *S. invicta*. Critical environmental factors such as temperature, precipitation, and topography significantly influence the establishment, reproduction, population, and expansion of *S. invicta* colonies (Song et al., 2021). Optimal temperature ranges enhance queen fecundity, promote brood development, and increase worker activity, thereby facilitating rapid colony growth and the exploitation of new habitats (Porter, 1988; Queffelec et al., 2021). Moderate, seasonally distributed rainfall increases soil moisture, facilitates nest construction, and boosts foraging activity, while adequate humidity also improves foraging efficiency and larval survival. However, excessive rainfall poses a threat to colony survival by increasing the risk of flooding (Ward, 2009; Li et al., 2023; Khan et al., 2025). Precipitation influences the survival and distribution of *S. invicta* by supporting nest building and brood development when sufficient but disrupting colonies and foraging behavior when levels are too low or too high (Morrison et al., 2004; Mertl et al., 2009). *S. invicta* predominantly invades regions with annual precipitation exceeding 500 mm, suggesting that rainfall is a critical determinant of its distribution (Li et al., 2023). Therefore, the empirical evaluation of key bioclimatic indicators is essential for determining the potential invasion range of *S. invicta*, as these indicators reflect significant temperature and moisture parameters that influence its survival and proliferation (Wang et al., 2022; Tang et al., 2025).

Climatic factors, such as temperature and precipitation, are commonly employed to predict the current and future distribution of *S. invicta* worldwide. However, edaphic factors, particularly soil properties, may significantly constrain settlement and colony expansion, although research on the latter has been reported yet. Infestation by *S. invicta* initially alters soil properties (Xi et al., 2010), with subsequent studies examining reductions in nitrogen and phosphorus, alongside increases in potassium and shifts in acidity (Shi et al., 2023). These are expected to disrupt nutrient cycling and affect soil biota, suggesting that soil also plays a crucial role in regulating the distribution, diversity, and success of ant colonies by influencing trophic resources, i.e., soil arthropod prey, and nest-site thermodynamics. Similarly, studies have shown that soil organic carbon serves as a key indicator of soil and ecosystem productivity (Sanabria et al., 2014; Peters et al., 2016; Perfecto & Philpott, 2023). Equally, studies demonstrated that soil pH (in water) can directly and indirectly influence ant community composition (Stark et al., 2012; Dauber & Wolters, 2000; Frouz et al., 2003). *S. invicta* inhabits disturbed and open environments; therefore, soil pH can determine its competitiveness with local ant fauna and its adaptability for brood development (Peters et al., 2016; Travanty, 2021). Additionally, soils with balanced proportions of sand and silt promote optimal aeration and drainage, thereby creating favorable nesting environments for ground-dwelling ant species (Song et al., 2021). Furthermore, vegetation cover and land surface temperature (LST) are key factors affecting habitat suitability (Li et al., 2023). Elevated normalized difference vegetation index (NDVI) values generally signify increased resource availability and enhanced microclimatic stability, which collectively enhance foraging efficiency and successful colony establishment. Similarly, increased LST can alter the thermal environment, influencing the metabolic rates and activity patterns of the species, which is crucial for colony success and expansion. Topographic variation alters local temperature and moisture conditions, generating microhabitats that either promote or restrict colony persistence (Vogt et al., 2008; Morgan & Guénard, 2019).

Modeling tools such as Maximum Entropy Modeling (MaxEnt) and Generalized Linear Models (GLMs) integrate different variables to delineate potential risk areas and identify regions and variables that are most suitable for invasion (Phillips et al., 2006). These models offer essential guidance for designing region-specific management strategies, optimizing monitoring networks, and prioritizing early interventions (Song et al., 2021). Global warming expands thermally suitable zones and alters precipitation patterns. Model-based forecasting becomes increasingly important for anticipating the spread of *S. invicta* and for implementing effective, climate-responsive control and management programs (Chen et al., 2019; Li et al., 2023).

Previous studies have predicted the current and potential distribution of RIFA primarily using bioclimatic variables, particularly temperature and precipitation. However, the potential influence of land physical properties and soil-related factors has received no attention in ecological niche modeling (Morrison et al., 2004; Sutherst & Maywald, 2005; Sung et al., 2018; Wang et al., 2022; Li et al., 2023; Tang et al., 2025). Incorporating soil variables, such as soil

organic carbon and soil water pH, may improve predictions of habitat suitability, as these factors can influence microhabitat conditions, nesting suitability, and local environmental constraints that shape the invasion dynamics of *S. invicta*. In this study, we applied MaxEnt and generalized linear models (GLM) to evaluate the potential distribution of RIFA in China and assess the relative influence of climatic and soil-related variables using updated environmental datasets and comprehensive occurrence records. The principal objectives are to (1) identify the critical determinants influencing the spatial distribution of *S. invicta* and (2) investigate potential niche shifts of *S. invicta* during the Current (1970–2000) and future climate change scenarios. This integrative analysis aims to enhance the ecological characterization of *S. invicta*, thereby informing the formulation of targeted, effective, and comprehensive strategies to reduce its invasive potential and ecological effects in China.

2. MATERIAL AND METHODS

2.1. Species distribution record

The distribution record for *S. invicta* was taken from the following resources: the Global Biodiversity Information Facility (GBIF, https://www.gbif.org/), using the package "rgbif" (Chamberlain et al., 2022); iNaturalist (https://www.inaturalist.org/), using the package "rinat" (Barve & Hart, 2017); AntWeb (https://www.antweb.org/); and the Ministry of Agriculture and Rural Affairs of the People's Republic of China (https://www.moa.gov.cn/). The above-mentioned databases were accessed on 9 September 2025. We used Google Earth (https://earth.google.com/) to locate the sites without coordinates. We compiled 1,610 distribution records (Fig. 1). Spatially autocorrelated distribution points create environmental biases in the models, necessitating data rarefaction (Veloz, 2009). The R package "spThin" was used to thin the collected datasets (distance < 5 km) to decrease spatial autocorrelation (Aiello-Lammens et al., 2015). Consequently, this study used 965 occurrence points for further analysis. The density occurrence map of *S. invicta* was generated in R v4.4.3 (R Core Team, 2016) using the ggplot2 package (Wickham et al., 2016).

2.2. Environmental variables

Understanding the factors influencing *S. invicta* habitat is crucial for predicting its ecological adaptability, colony dynamics, and rapid dispersal. Therefore, in this study, we used bioclimatic and elevation data, accessed from WorldClim website (http://www.worldclim.org/), with a spatial resolution of 2.5′ (~4.3 km). The topographic values were calculated from the elevation raster layer using the "terrain" function from the raster package in R v4.4.3 (Hijmans, 2025). Furthermore, 14 variables were downloaded from the International Soil Reference and Information Center (ISRIC, https://soilgrids.org/) with a spatial resolution of 250 m. Additionally, 5 environmental variables were retrieved from the Google Earth Engine (GEE, https://earthengine.google.com/) with a spatial resolution of 1000 m (1 km). The spatial resolution of all variables was set to 2.5′ (~4.3 km), using the package "terra" (Hijmans, 2020). All variables are classified and listed in Table S1. Variables downloaded from the GEE database were only used in generalized linear models (GLMs) due to lack of data across different periods.

Correlation and principal component analysis (PCA) were conducted to assess the correlation among the 34 variables, using the "cor" function (Wei et al., 2017) in R v4.4.3 (R Core Team, 2016), which was used in the initial MaxEnt model (Table S2) . We assumed that topography and soil-related variables remained constant in the future, except for bioclimatic variables, because changes in these variables lag significantly behind climate change (Fan et al., 2022; Zhan et al., 2022). The selection criteria for the final MaxEnt model involved retaining the most significant variables that demonstrated substantial contribution outcomes among pairs of highly associated variables ($|r| \geq 0.8$) (Hussain et al., 2025, 2026). Therefore, this study selected only seven variables for the final MaxEnt model. These factors are Bio2 (mean diurnal range), Bio10 (mean temperature of warmest quarter), Bio11 (mean temperature of coldest quarter), Bio14 (precipitation of driest month), topography, water pH, and soil organic carbon (Table 1).

Table 1. Percent (%) contributions of 7 most important bioclimatic variables used in the final maxent model for *S. invicta*.

Variable	Variable description	Contribution (%)
Bio14	Precipitation of driest month	45.2
Bio11	Mean temperature of coldest quarter	21.4
Bio10	Mean temperature of warmest quarter	10.4
pH water	—	10.1
Topography	—	8.2
Bio2	Mean diurnal range	4.2
Soil organic carbon	—	0.4

2.3. Modeling and evaluation

The "ENMeval" package v2.0.5.2 (Muscarella et al., 2014) was used to evaluate the performance and complexity of the MaxEnt model v3.4.4 (Phillips et al., 2006) in R v4.4.3 to reduce model overfitting by conducting a tuning exercise by testing a set of regularization multiplier values (1, 2, 3) and feature class combinations [linear (L), quadratic (Q), product (P), threshold (T), and hinge (H)]. Regularization multiplier (RM) value (1–3) with intervals of 1, combined with the feature classes (L, LQ, H, LQH, LQHP, and LQHPT) (Hussain et al., 2025, 2026). The final model was selected based on the lowest delta Akaike information criterion (AICc) values using "block" (Hussain et al., 2025, 2026). The model with features LQHP and an RM of 1 (Fig. S1) was selected for the MaxEnt model because it provided the best balance of fit and parsimony.

Twenty-five percent of the total points were selected for testing, while the remaining 75% were kept for training. Overall, 10,000 background points were chosen (Su et al., 2023; Hussain et al., 2025, 2026). We used the "terra" package in R v4.4.3 to keep the historical and future bioclimatic variables (only Bio2, Bio10, and Bio11) on the same scale (Hijmans, 2020; Hussain et al., 2025). The continuous model output was converted into a binary classification to define risk zones using the threshold that maximizes the sum of sensitivity and specificity. Risk zones were categorized into the following four levels: negligible-risk areas (0.00–0.0274), low-risk areas (0.0275–0.30), medium-risk areas (0.30–0.60), and high-risk areas (0.60–1.00) (Wang et al., 2023). The area corresponding to each risk class was calculated in 10^6 km^2 (million km^2) (Hussain et al., 2025, 2026). Model predictive performance was assessed using two metrics. Areas under the Receiver Operating Characteristic (ROC) curves were produced with Area Under the Receiver Operating Characteristic Curve (AUC) metrics, averaged with ten replicated runs, and used for model assessment along with the True Skill Statistic (TSS) (Su et al., 2023; Hussain et al., 2025, 2026).

2.4. Future projections

Future climate data were derived from CMIP5 projections, as outlined in the fifth IPCC report. Two global climate models (GCMs) – ACCESS1-0 and BCC-CSM1-1 (Collier & Uhe, 2012; Ren et al., 2016) for the 2050s (average for 2041–2060) and 2070s (average for 2061–2080) – were selected due to their better performance. The risk areas were predicted based on future climate data with an intermediate condition (RCP4.5) (Su et al., 2023; Hussain et al., 2025). The risk areas associated with varying climate conditions were computed utilizing the "terra" package in R v4.4.3 (Hijmans, 2020).

2.5. Statistical analysis

To assess species-environment correlations, we applied three generalized linear model (GLM) link functions – logit, probit, and complementary log-log (cloglog) – to evaluate their efficacy, alongside a quadratic model incorporating squared components of all predictors to account for any non-linear environmental influences (Bonate, 2011; Dawotola & Tasdan, 2024). All factors were normalized using z-scores (Su et al., 2023), and pseudo-absences (n = 2 × number of presences) were randomly sampled via the "spatSample()" function (Capó et al., 2023). Model performance was evaluated using the delta AICc (Warren et al., 2014). The model (quad) with the minimal AICc value was chosen as the optimal fitting model (Fig. S2).

RESULTS

The occurrence density map (Fig. 1) confirmed that *S. invicta* is widely spread in southern China, particularly in Taiwan Island and Guangdong, Fujian, Jiangxi, Guangxi, and Yunnan Provinces.

3.1. MaxEnt modeling of *S. invicta*

3.1.1. Model efficiency and factor role

The models for *S. invicta* achieved an average Area Under the Receiver Operating Characteristic Curve (AUC) of 0.928 (Fig. S3a) and a True Skill Statistic (TSS) of 0.887, demonstrating excellent predictive performance. The average omission and predicted area curves showed

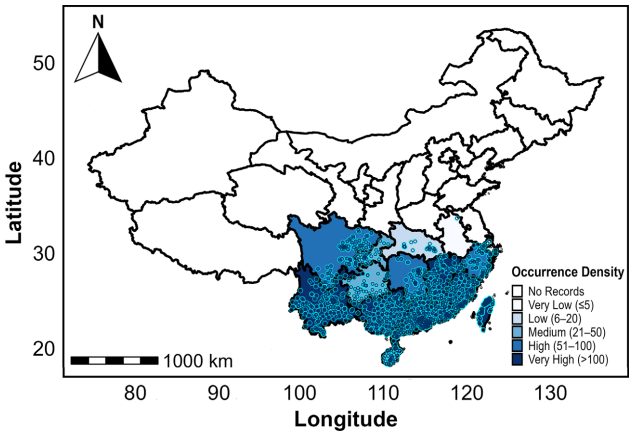

Fig. 1. Occurrence density map of *S. invicta* across China. The color legend shows *S. invicta* occurrence density per province. This map has been cropped to include only regions with known infestations to improve the visual clarity of the data.

that the predicted omission rate closely matches the average omission rate, further highlighting the model's higher execution (Fig. S3b). Based on the Jackknife test, soil organic carbon showed the lowest gain when used alone and the least drop when removed (Fig. 2). The response curves showed a high occurrence chance of *S. invicta* when precipitation of driest month (Bio14) was above 20 mm, mean temperature of coldest quarter (Bio11) was above 5°C, temperature of warmest quarter (Bio10) was above 25°C, water pH was around 0, topography was from 0 to 0.1, mean diurnal range (Bio2) was around 6°C, and soil organic carbon was less than 500 (Fig. 3). This indicates that *S. invicta* prefers warm, humid, plain areas and acidic water. The percentage of seven most influential factors used in the final MaxEnt model were Bio14 (45.2%), Bio11 (21.4%), Bio10 (10.4%), water pH (10.1%), topography (8.2%), Bio2 (4.2%), and soil organic carbon (0.4%) (Table 1).

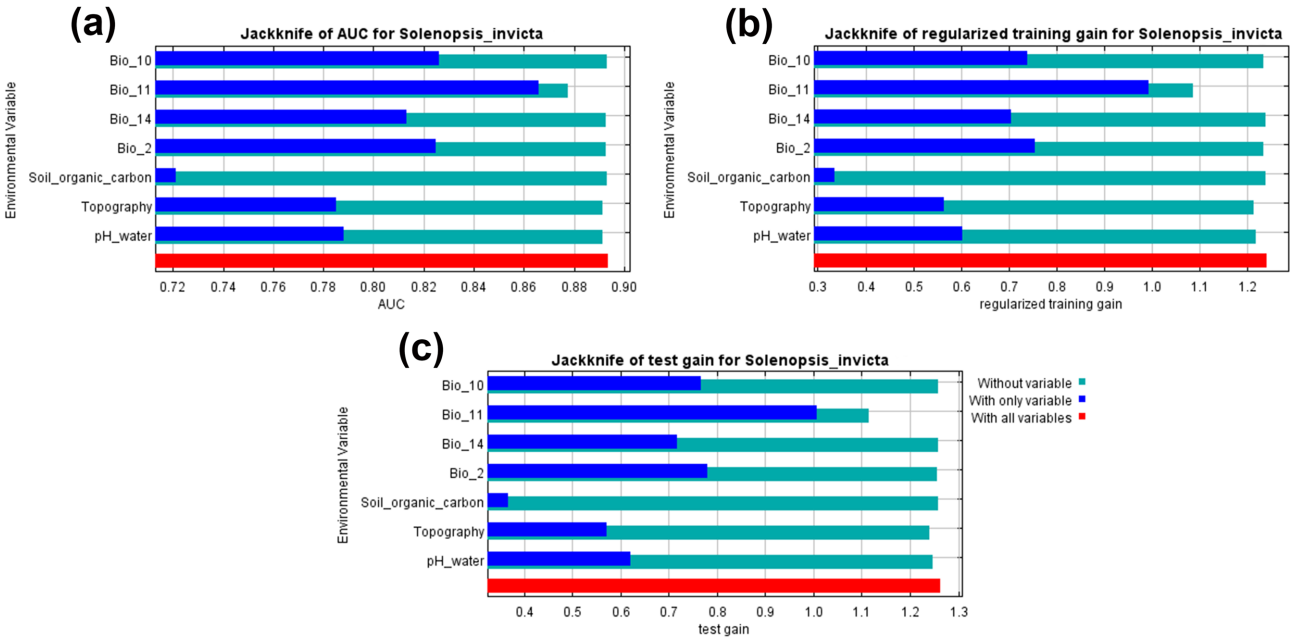

Fig. 2. Jackknife analysis output for the seven most important variables: (a) AUC values; (b) regularized training gain; and (c) test gain.

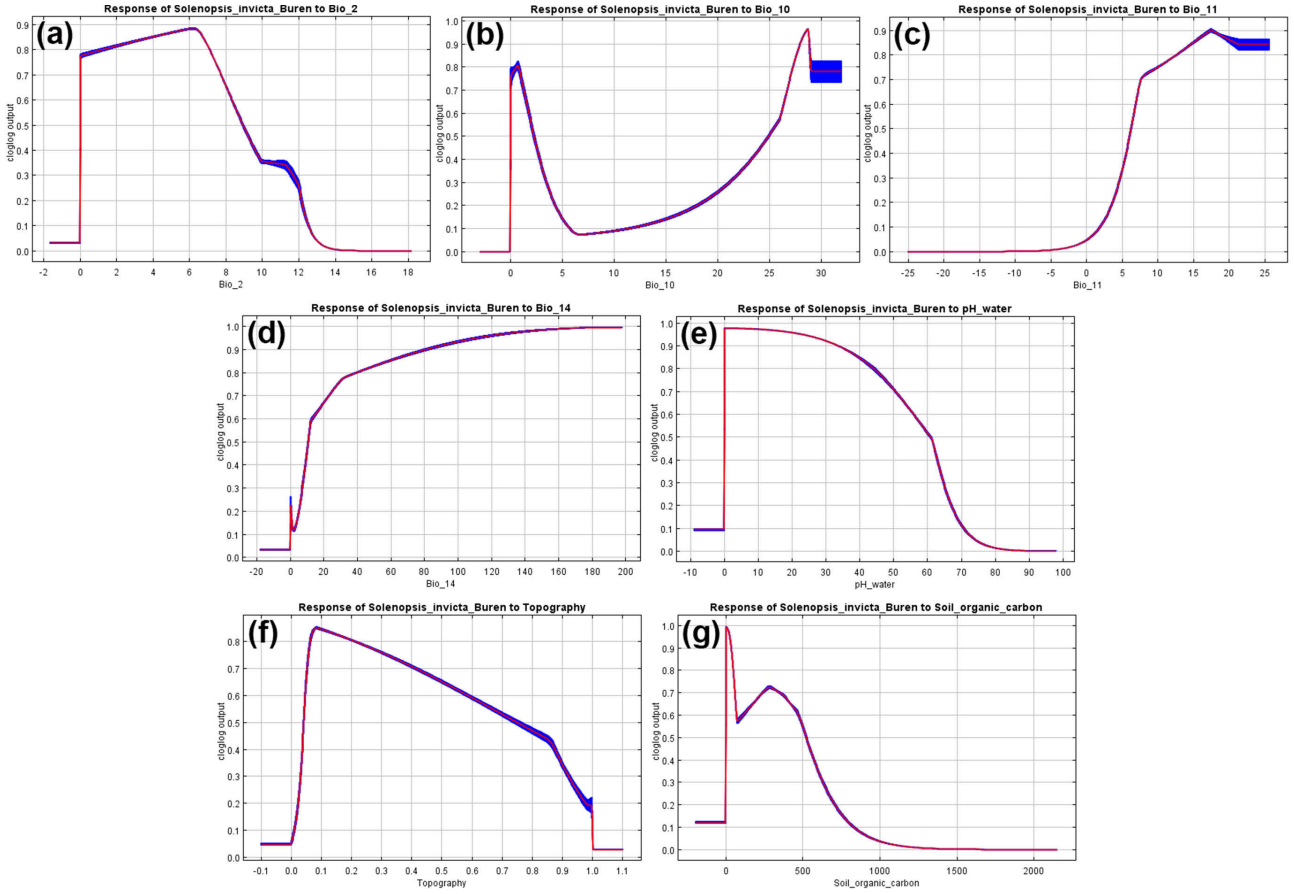

Fig. 3. Response curves of the seven most important variables for *S. invicta*.

3.2. Risk area under current (1970–2000) climate scenarios

Based on 1970–2000 bioclimatic variables, the risk areas of *S. invicta* were found throughout southern China. The high-risk areas are mainly located in Taiwan and Hainan Island, as well as Yunnan, Guangxi, Guangdong, Fujian, Sichuan, Hunan, and Jiangxi provinces (Fig. 4). Under 1970–2000 environmental scenarios, the total risk area of *S. invicta* was 2.554 million km², accounting for 27.52% of the entire land area. High-, moderate-, and less-risk zones accounted for 27%, 35.71%, and 37.27% of the total risk zones, respectively (Table 2).

3.3. Future risk areas under global warming conditions

Future risk areas associated with climate change conditions are increasing relative to the predicted suitable regions for *S. invicta* in China under 1970–2000 climatic conditions. Fig. 5a–d shows the suitable areas for *S. invicta* under climate change scenarios in the 2050s and 2070s. The total risk area was 2.976 and 2.925 million km² in the 2050s under ACCESS1-0 and BCC-CSM1-1 scenarios, respectively (Table 2). The total risk area is expected to increase further to 3.056 and 2.941 million km² under the ACCESS1-0 and BCC-CSM1-1 scenarios, respectively (Table 2). The high-risk area was 1.275 (1.85-fold greater than 1970–2000) and 1.099 (1.59-fold greater than 1970–2000) million km² in 2050 under the ACCESS1-0 and BCC-CSM1-1 scenarios, respectively. As compared to the Current period, in the 2070s, the high-risk areas are expected to increase further to 1.185 million km² (1.72 times > than 1970–2000) under the ACCESS1-0 and 1.161 million km² (1.68 times > than 1970–2000) under the BCC-CSM1-1 scenarios (Table 2).

3.4. Non-linear species-environment relationships

To account for any non-linear ecological responses, we employed a GLM that included both linear and quadratic terms for all predictors. Generalized linear models indicate that variables including organic carbon density, volumetric water content at –10 kPa, topography, and the NDVI ex-

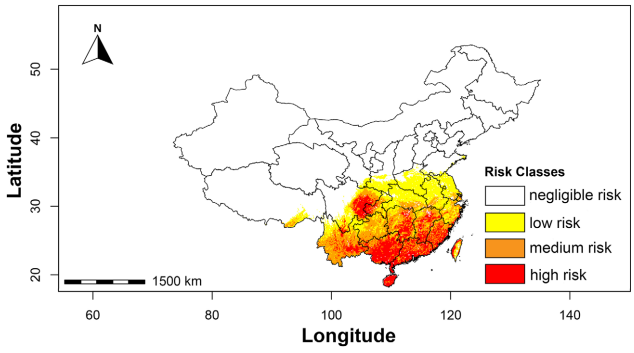

Fig. 4. Current (averaged from 1970–2000) suitable area of *S. invicta* in China. This map has been cropped to include only areas with known infestations to improve the visual clarity of the figure.

Table 2. Predicted risk area of *S. invicta* across China under 1970−2000 and future climate scenarios, calculated in 10^6 km^2.

Habitat suitability	Current (1970−2000)	Global warming scenarios			
		RCP4.5 2050s	RCP4.5 2070s	RCP4.5 2050s	RCP4.5 2070s
GCM	Current	ACCESS1-0	ACCESS1-0	BCC-CSM1-1	BCC-CSM1-1
Area	10^6 km^2	10^6 km^2	10^6 km^2	10^6 km^2	10^6 km^2
Negligible risk	6.729	6.522	6.443	6.573	6.558
Less risk	0.952	0.824	0.908	0.821	0.775
Moderate risk	0.912	0.877	0.963	1.005	1.005
High risk	0.690	1.275	1.185	1.099	1.161
Total risk area	2.554	2.976	3.056	2.925	2.941

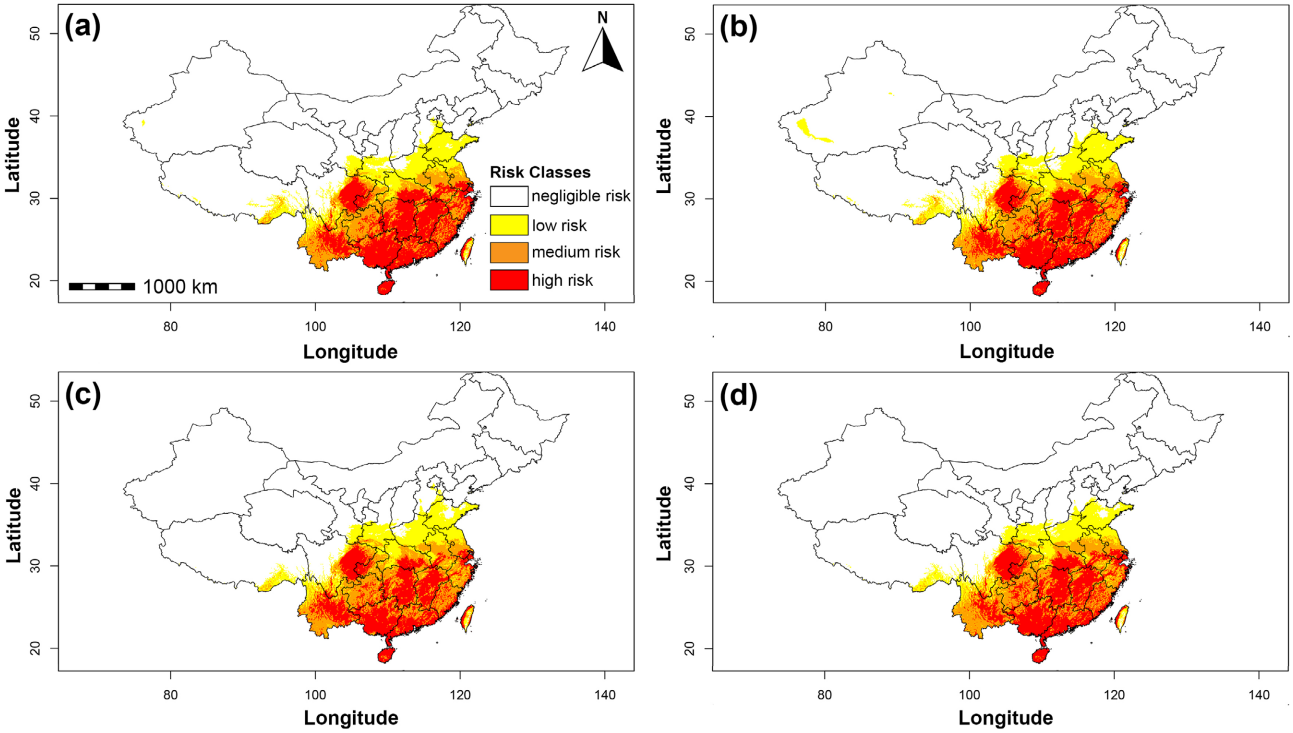

Fig. 5. Risk area of *S. invicta* in China under two global climate models, ACCESS1-0 for (a) 2050s-RCP4.5; (b) 2070s-RCP4.5, and BC-CCSM1-1 for (c) 2050s-RCP4.5; and (d) 2070s-RCP4.5. This map has been cropped to include only regions with known infestations to improve the visual quality of the figure.

hibited significant linear and quadratic relationships, suggesting a unimodal (hump-shaped) response, with intermediate levels of these variables associated with heightened probabilities of *S. invicta* occurrence. Moreover, elements such as elevated urbanization, increased volumetric water content at –1500 kPa, and moderate clay content increase the likelihood of *S. invicta* occurrences. Additionally, both linear and quadratic terms demonstrate that the probability of species occurrence increases with rising land surface temperature. The likelihood of species occurrence decreases with significant increases in soil organic carbon, sand, silt, and water pH (Table S1). Overall, the species predominantly prefers warm areas characterized by moderate soil moisture, organic carbon, vegetation cover, topographic diversity, and increased urbanization, although harsh soil conditions typically limit its appropriate ranges.

4. DISCUSSION

The global spread of RIFA represents a major ecological and socio-economic concern. As with many invasive species, its most immediate impact is the displacement of native fauna and the disruption of local ecosystems, posing a serious threat to native biodiversity. In addition, *S. invicta* is highly aggressive and capable of delivering painful stings, which can lead to significant public health concerns for humans and domestic animals. The combined effects of biodiversity loss, medical risks, and agricultural damage ultimately translate into substantial economic costs associated with management, healthcare, and control efforts. The expansion of *S. invicta* is expected to intensify under ongoing global warming, increasing international trade, and growing human mobility, all of which facilitate its introduction and establishment in new regions (Vinson, 1997; Ascunce et al., 2011). The species has demonstrated remarkable invasive capacity, as evidenced by its rapid colonization and extensive spread across the United States, where its wide distribution has made eradication efforts particularly challenging (Steele et al., 2020). In China, *S. invicta* was first reported in Guangdong and has since expanded into several additional provinces, highlighting its

strong dispersal ability and potential for continued range expansion (Zeng et al., 2005).

Since 2013, the geographic range of RIFA has expanded markedly in China, with the number of affected cities increasing by 71.43% and the number of affected counties increasing by 165.09% across multiple provinces (Du et al., 2007; Wang et al., 2022). These increases reflect a substantial expansion in the recorded distribution of RIFA, indicating its rapid spread into new administrative regions. Therefore, strengthening the inspection system and monitoring the transportation of goods is crucial. The projected growth in medium- and low-risk zones highlights the importance of integrated management, early detection, and enhanced international collaboration to reduce future impacts.

Temperature is the main climatic factors influencing *S. invicta* because of their direct effects on physiology and ecology. Cool, dry conditions generally limit colony establishment by reducing metabolic activity, hindering foraging, and significantly affecting the development, survival, and behavior of *S. invicta* (Ward, 2009; Li et al., 2023; Wang et al., 2023). Similarly, low temperatures reduce foraging activity and nutrient acquisition while also delaying brood development, thereby constraining colony growth and recovery (Roeder et al., 2018; Lei et al., 2021). This suggests that cool climates serve as an important barrier to colonization because colonies cannot sustain the reproductive output required for long-term population persistence. Although an increase in temperature can increase biotic activity, and exacerbate the effects of desiccating stress, especially when combined with a decrease in humidity.

Like temperature, precipitation mainly influences habitat suitability by affecting soil water and nest stability. Moderate rainfall (typically over 510 mm annually) maintains soil moisture sufficient to prevent brood desiccation, aid tunnel construction, and support plants that feed honeydew-producing insects, a crucial food source (Morrison et al., 2004; Li et al., 2023). Insufficient rainfall results in dry conditions that dry out nests and diminish food supplies, leading populations to move toward water-rich areas such as riparian zones or irrigated lands. Excessive rainfall, however, increases the risk of flooding nests, drowning broods, and incurring costly relocations. Continuous surface wetness also hampers foraging and disrupts trail pheromone signaling (Mertl et al., 2009). Thus, the rainfall range establishes a soil moisture window that creates a suitable habitat, with arid conditions at one end and flood risk at the other. These climatic factors do not operate in isolation. Topography influences local conditions by altering microclimates – slope and aspect impact soil temperature and drainage, which interact with regional rainfall to form a mosaic of microhabitats (Morgan & Guénard, 2019). Therefore, well-drained slopes can reduce the adverse effects of heavy rain, while north-facing slopes in cooler regions may be too cold. Ultimately, the distribution of *S. invicta* depends on the combination of thermal conditions that support vital biological activities and hydrologic factors that maintain stable nest structures and effective foraging.

Comparative analyses reveal that the climatic thresholds used in this study align with the geographic distribution of *S. invicta* in China. In southern China, warm weather supports wet conditions, and it is projected that global warming will enable the *S. invicta* population to expand from south to north (Sutherst & Maywald, 2005; Duan et al., 2021). Rising temperatures will create a more suitable environment for their survival and growth (Porter, 1988; Roeder et al., 2018,), increasing the likelihood of range expansion into northern regions (Xu et al., 2009). Expected climatic shifts will ease these constraints and boost invasion potential, highlighting the importance of ongoing climate-based monitoring and flexible management strategies.

Based on the ensemble consensus of the MaxEnt model, the extent of potential RIFA distribution during the Current period (1970–2000) was estimated at 2.555 million km², accounting for over one-quarter (27.52%) of China's land surface. High-, moderate-, and less-risk habitats accounted for 27%, 35.71%, and 37.27% of the total risk areas, respectively. These findings align with earlier research indicating that temperature, precipitation, and topography are the main environmental factors influencing habitat suitability for *S. invicta* (Morgan & Guénard, 2019; Li et al., 2023). In the future, the risk area for *S. invicta* is predicted to expand to roughly 3 million km² by 2050–2070 under ACCESS1-0 and BCC-CSM1-1 scenarios. High-risk zones are expected to increase 1.6–1.9 times compared to the 1970–2000 baseline. The prevalence of moderate- and high-risk zones, which together account for over 62.7% of the suitable area, likely indicates regions where temperature (e.g., sufficient warmth for brood development) and precipitation (e.g., sufficient moisture for nest stability) align with the species' optimal conditions. In contrast, low-risk zones may indicate areas where one or more of these factors are near a critical threshold, thereby limiting population growth. The strong agreement between modeled high-risk zones and documented infestations indicates that the model accurately represents *S. invicta's* realized niche. Climate driven poleward expansion of invasive species, including fire ants, has been well documented (Sung et al., 2018), and MaxEnt projections suggest a high probability of further habitat expansion under global warming conditions (Sung et al., 2018, Li et al., 2023). Many high-suitability regions are densely populated and heavily used for agriculture, which increases propagule pressure from trade, transportation, and soil translocation.

The distribution of *S. invicta* in China is influenced by a hierarchy of environmental factors, with precipitation being the primary factor limiting its distribution. Specifically, precipitation of driest month (Bio14) is important for defining the arid boundaries of its range, especially in northwestern China. Having a specific dry-season moisture pattern is vital, as it allows colonies to access soil moisture for hydration, reducing desiccation stress and helping them survive in otherwise dry areas (Ward, 2009; Wang et al., 2023; Tang et al., 2025). Following precipitation, temperature is the next key factor. The role of mean temperature of coldest quarter (Bio11) highlights that brood develop-

ment stops below a critical thermal threshold, increasing colony mortality and essentially defining the northern limit of invasion (Ward, 2009; Wang et al., 2023; Tang et al., 2025). Conversely, mean temperature of warmest quarter (Bio10) shows that adequate summer warmth is necessary to support high rates of colony growth, reproduction, and alate flight activity, which are vital for population spread and new colony foundation. Additionally, mean diurnal range (Bio2) affects daily activity; a moderate variation of around 6°C provides a stable thermal environment, enabling predictable foraging and lowering metabolic stress (Ward, 2009; Wang et al., 2023; Tang et al., 2025). Beyond these macroclimatic variables, soil organic carbon modifies habitat suitability at a local scale. Higher soil organic carbon likely enhances colony establishment by improving soil structure for nesting and increasing the availability of nutrients that support the ant's trophic interactions, such as cultivating mutualistic insects. Finally, the soil water pH interacts with these factors to shape the subterranean environment. Soil pH influences microbial community composition and the solubility of essential nutrients and minerals, thereby indirectly affecting brood development and overall colony health by altering food resource quality and availability. The ideal niche is primarily found in the warm, humid, and thermally stable areas of southern China, where favorable rainfall, temperature patterns, and soil conditions converge. In contrast, colder northern regions, arid northwestern areas, and high-altitude zones lack the moisture, warmth, and soil chemistry thresholds necessary for *S. invicta* to establish a stable population.

Specifically, increasing minimum temperature of coldest month (Bio6) and mean temperature of coldest quarter (Bio11) are expected to lift cold thermal barriers that currently limit their northern and high-altitude distribution, allowing colonies to establish and thrive in previously unsuitable areas. Meanwhile, changes in precipitation patterns, including altered dry-season moisture, may reduce water stress in some regions, further enlarging suitable habitats. These findings support earlier work showing the progressive increase of high-risk areas under future climate change scenarios (Wang et al., 2023). The global temperature is rising roughly about 0.2°C per decade, with an anticipated increase of 0.8–1.1°C (according to BCC-CSM1-1 forecasts) in China by 2050 (Zhao et al., 2022), creating conditions conducive to range expansion. These projections align with Wang et al. (2022), who predict significant habitat expansion in southern China by the 2070s. Collectively, the evidence demonstrates that climate change will accelerate the spread of *S. invicta* populations across China, heightening ecological and economic threats. The non-linear associations with land surface temperature and NDVI indicate that extreme heat and dense vegetation also affect colony proliferation. This supports the hypothesis that *S. invicta* thrives best under moderate environmental conditions.

Effective long-term management of RIFA in China requires coordinated, science-based strategies that integrate ecological considerations. Regional coordination and targeted interventions can help prevent reinfestation and optimize resource use, while environmentally safe control methods, such as parasitic phorid flies, nematodes, and entomopathogenic fungi, offer promising biocontrol options (Zhang et al., 2020, Pires et al., 2022). Habitat modifications, including soil pH adjustment and organic matter management, can further reduce the likelihood of colony establishment and expansion (Wolters, 2000, Pearsons & Tooker, 2017). The integration of innovative monitoring technologies, such as AI-assisted detection, can support rapid, data-driven responses (Chaudhary & Jabborova, 2026). Although management was not the primary focus of this study, these recommendations, drawn from existing research, highlight practical avenues to mitigate the spread of RIFA and protect agricultural productivity, biodiversity, and public welfare.

5. CONCLUSION

This research examined the distribution of *S. invicta* and its associations with 39 environmental variables. *S. invicta* is prevalent in southern China, particularly in Taiwan Island and Guangdong, Fujian, Jiangxi, Guangxi, and Yunnan Provinces. The MaxEnt model was employed to predict the potential risk areas of *S. invicta* during the Current period and under future global warming scenarios, utilizing seven predominant factors mean diurnal range (Bio2), mean temperature of warmest quarter (Bio10), mean temperature of coldest quarter (Bio11), precipitation of driest month (Bio14), topography, water pH, and soil organic carbon. Bio14 and Bio11 were the most important factors in the model, accounting for 66.6% of the explained variance and primarily influencing the spread of RIFA, followed by Bio10, water pH, topography, Bio2, and soil organic carbon. According to the simulation results under global warming scenarios BCC-CSM1-1 and ACCESS1-0 for the years 2050 and 2070, the risk areas of *S. invicta* are expected to increase, followed by a northward expansion. Factors including high land surface temperature and moderate soil moisture, organic carbon, vegetation cover, and topographic diversity, together with increased urbanization, facilitate the spread of *S. invicta,* however, harsh soil conditions often limit its suitable range. These findings offer essential insights for forecasting and controlling the spread of *S. invicta* in China. Effective management of RIFA relies on integrating broadcast baits with insect growth regulators, targeted nest injections, and environmentally friendly physical methods, such as cryotherapy and high-temperature steam, and is supported by ongoing surveillance and public engagement. This study endorses wider efforts in pest control and ecological management.

ACKNOWLEDGEMENTS. We gratefully acknowledge the support of W. Javaid and G. Li for materials, methodological guidance, and translations.

AUTHORS' CONTRIBUTIONS. Haroon: Conceptualization, data curation, formal analysis, investigation, methodology, visualization, writing – original draft, writing – review and editing. R. Hussain: Formal analysis, validation, visualization, writing – review and editing. C. Wang: writing – original draft, project ad-

ministration, writing – review and editing. S. Zhang: validation, writing – review and editing, project administration.

DATA AVAILABILITY STATEMENT. The data supporting the findings of this study are available in the supplementary data files.

CONFLICT OF INTEREST. The authors declare no conflicts of interest.

REFERENCES

Aiello-Lammens M.E., Boria R.A., Radosavljevic A., Vilela B. & Anderson R.P. 2015: spThin: an R package for spatial thinning of species occurrence records for use in ecological niche models. — *Ecography* **38**: 541–545.

Ascunce M.S., Yang C.-C., Oakey J., Calcaterra L., Wu W.-J., Shih C.-J., Goudet J., Ross K.G. & Shoemaker D. 2011: Global invasion history of the fire ant *Solenopsis invicta*. — *Science* **331**: 1066–1068.

Barve V. & Hart E. 2017: *rinat: Access iNaturalist Data Through APIs. R Package.* URL: https://CRAN.R-project.org/package=rinat.

Bonate P.L. 2011: *Pharmacokinetic-Pharmacodynamic Modeling and Simulation.* Springer, New York, 637 pp.

Bradshaw C.J., Leroy B., Bellard C., Roiz D., Albert C., Fournier A., Barbet-Massin M., Salles J.-M., Simard F. & Courchamp F. 2016: Massive yet grossly underestimated global costs of invasive insects. — *Nature Commun.* **7**: 12986, 8 pp.

Capó M., Cortés-Fernández I. & Borràs J. 2023: Preprint. Spatial distribution of insular cliff vegetation and future scenarios in a climate change perspective. — *bioRxiv* URL: https://doi.org/10.1101/2023.11.09.566357, 25 pp.

Chaudhary M. & Jabborova D. 2026: Smart sensing technologies: Monitoring insect pests with AI. In Mitra D., Pellegrini M. & Sierra B.E.G. (eds): *Advancements in Entomology: Bridging Forensic Science and Sustainable Agriculture.* Springer, Singapore, pp. 423–440.

Chamberlain S., Oldoni D. & Waller J. 2022: *rgbif: Interface to the Global Biodiversity Information Facility API.* URL: https://github.com/ropensci/rgbif.

Chen C., Harvey J.A., Biere A. & Gols R. 2019: Rain downpours affect survival and development of insect herbivores: the specter of climate change? — *Ecology* **100**: e02819, 10 pp.

Collier M. & Uhe P. 2012: *CMIP5 Datasets from the ACCESS1. 0 and ACCESS1. 3 Coupled Climate Models.* Centre for Australian Weather and Climate Research, Aspendale, 32 pp.

Dauber J. & Wolters V. 2000: Microbial activity and functional diversity in the mounds of three different ant species. — *Soil Biol. Biochem.* **32**: 93–99.

Dawotola T.B. & Tasdan F. 2024: A comparative analysis of some link functions for binomial regression models with applications to bioassay data. — *Int. J. Sci. Res. Modern Technol.* **3**: 106–116.

Du Y.Z., Gu J., Guo J.B., Dai L., Ju R.T. & Hu X.N. 2007: Study on the potential distribution area of invasive alien pest red imported fire ant, *Solenopsis invicta* Buren in China. — *Sci. Agric. Sin.* **40**: 99–106.

Duan R., Huang G., Li Y., Zheng R., Wang G., Xin B., Tian C. & Ren J. 2021: Ensemble temperature and precipitation projection for multi-factorial interactive effects of GCMs and SSPs: application to China. — *Front. Environ. Sci.* **9**: 742326, 12 pp.

Fan Z.F., Zhou B.J., Ma C.L., Gao C., Han D.N. & Chai Y. 2022: Impacts of climate change on species distribution patterns of *Polyspora* sweet in China. — *Ecol. Evol.* **12**: e9516, 24 pp.

Frouz J., Holec M. & Kalčík J. 2003: The effect of *Lasius niger* (Hymenoptera, Formicidae) ant nest on selected soil chemical properties. — *Pedobiologia* **47**: 205–212.

Gutrich J.J., VanGelder E. & Loope L. 2007: Potential economic impact of introduction and spread of the red imported fire ant, *Solenopsis invicta*, in Hawaii. — *Environ. Sci. Policy* **10**: 685–696.

Hijmans R.J. 2025: *raster: Geographic data analysis and modeling. R package Version 517, Vol. 2.* pp. 2–12. URL: https://CRAN.R-project.org/package=raster.

Hijmans R.J. 2020: *terra: Spatial data analysis*. *CRAN: Contributed Packages*. URL: https://CRAN.R-project.org/package=terra.

Huang D.C., Chou Y.C. & Tsou H.C. 2004: The occurrence and treatment of red imported fire ants in Taiwan. In: *Proceedings of the Symposium on the Control of FIFA*. Taiwan Forestry Research Institute, Taipei, pp. 1–13.

Hussain R., Miao P., Rehman A., Fang L., Xing L. & Hua Y. 2025: Species richness and spatial distribution of three Pieridae subfamilies across mainland China under past and future climates. — *Sci. Rep*. **15**: 45685, 14 pp.

Hussain R., Xing L. & Hua Y. 2026: Assessing the invasive risk of Rhinotermitidae in China under current and future global warming scenarios using the MaxEnt model. — *Front. Zool*. **23**: 10, 15 pp.

Jennings C. & McCubbin K. 2004: The national red imported fire ant eradication program overview. In: *Proceedings of the Symposium on the Control of FIFA*. Taiwan Forestry Research Institute, Taipei, pp. 70–100.

Khan S.A., Weemaels A.I., Liang M. & Guenard B. 2025: Ecological and environmental impacts of the Red Imported Fire Ants (*Solenopsis invicta*) in Mainland China, Hong Kong and Macau. — *Global Environ. Res.* **28**: 159–170.

Lei Y., Jaleel W., Shahzad M.F., Ali S., Azad R., Ikram R.M., Ali H., Ghramh H.A., Khan K.A. & Qiu X. 2021: Effect of constant and fluctuating temperature on the circadian foraging rhythm of the red imported fire ant, *Solenopsis invicta* Buren (Hymenoptera: Formicidae). — *Saudi J. Biol. Sci.* **28**: 64–72.

Li M., Zhao H., Xian X., Zhu J., Chen B., Jia T., Wang R. & Liu W. 2023: Geographical distribution pattern and ecological niche of *Solenopsis invicta* Buren in China under climate change. — *Diversity* **15**: 607, 17 pp.

Mertl A.L., Ryder Wilkie K.T. & Traniello J.F. 2009: Impact of flooding on the species richness, density and composition of Amazonian litter-nesting ants. — *Biotropica* **41**: 633–641.

Morgan B. & Guénard B. 2019: Local models reveal greater spatial variation than global grids in an urban mosaic: Hong Kong climate, vegetation, and topography rasters. — *Earth Syst. Sci. Data* **11**: 1083–1098.

Morrison L.W., Porter S.D., Daniels E. & Korzukhin M.D. 2004: Potential global range expansion of the invasive fire ant, *Solenopsis invicta*. — *Biol. Invas*. **6**: 183–191.

Muscarella R., Galante P.J., Soley-Guardia M., Boria R.A., Kass J.M., Uriarte M. & Anderson R.P. 2014: ENM eval: An R package for conducting spatially independent evaluations and estimating optimal model complexity for Maxent ecological niche models. — *Meth. Ecol. Evol.* **5**: 1198–1205.

Pearsons K.A. & Tooker J.F. 2017: In-field habitat management to optimize pest control of novel soil communities in agroecosystems. — *Insects* **8**: 82, 14 pp.

Perfecto I. & Philpott S.M. 2023: Ants (Hymenoptera: Formicidae) and ecosystem functions and services in urban areas: a reflection on a diverse literature. — *Myrmecol. News* **33**: 103–122.

Peters V.E., Campbell K.U., Dienno G., García M., Leak E., Loyke C., Ogle M., Steinly B. & Crist T.O. 2016: Ants and plants as indicators of biodiversity, ecosystem services, and conservation value in constructed grasslands. — *Biodiv. Conserv.* **25**: 1481–1501.

Phillips S.J., Anderson R.P. & Schapire R.E. 2006: Maximum entropy modeling of species geographic distributions. — *Ecol. Modell.* **190**: 231–259.

Pires D., Vicente C.S., Menéndez E., Faria J.M., Rusinque L., Camacho M.J. & Inácio M.L. 2022: The fight against plant-parasitic nematodes: Current status of bacterial and fungal biocontrol agents. — *Pathogens* **11**: 1178, 22 pp.

Porter S.D. 1988: Impact of temperature on colony growth and developmental rates of the ant, *Solenopsis invicta*. — *J. Insect Physiol.* **34**: 1127–1133.

Queffelec J., Allison J.D., Greeff J.M. & Slippers B. 2021: Influence of reproductive biology on establishment capacity in introduced Hymenoptera species. — *Biol. Invas.* **23**: 387–406.

R Core Team 2016: *R: A Language and Environment for Statistical Computing.* R Foundation for Statistical Computing, Vienna. URL: http://www. R-project. org/.

Ren H.-L., Wu J., Zhao C.-B., Cheng Y.-J. & Liu X.-W. 2016: MJO ensemble prediction in BCC-CSM1. 1 (m) using different initialization schemes. — *Atmospheric Oceanic Sci. Lett.* **9**: 60–65.

Roeder K.A., Roeder D.V. & Kaspari M. 2018: The role of temperature in competition and persistence of an invaded ant assemblage. — *Ecol. Entomol.* **43**: 774–781.

Sanabria C., Lavelle P. & Fonte S.J. 2014: Ants as indicators of soil-based ecosystem services in agroecosystems of the Colombian Llanos. — *Appl. Soil Ecol.* **84**: 24–30.

Schowalter T., Cooper K., Kramer K., Neely E., Ring D. & Ringe P. (eds) 2015: *Imported Fire Ant and Invasive Pest Ant Conference, April 6–8, 2015, New Orleans, Louisiana.* Albuquerque, NM, 89 pp.

Shi L., Liu F. & Peng L. 2023: Impact of red imported fire ant nest-building on soil properties and bacterial communities in different habitats. — *Animals* **13**: 2026, 22 pp.

Siddiqui J.A., Bamisile B.S., Fan R., Hafeez M., Islam W., Yang W., Wei M., Ran H., Xu Y. & Chen X. 2024: Ant invasion in China: An in-depth analysis of the country's ongoing battle with exotic ants. — *Ecol. Indicat.* **160**: 111811, 18 pp.

Silverman J. & Brightwell R.J. 2008: The Argentine ant: challenges in managing an invasive unicolonial pest. — *Annu. Rev. Entomol.* **53**: 231–252.

Song J., Zhang H., Li M., Han W., Yin Y. & Lei J. 2021: Prediction of spatiotemporal invasive risk of the red import fire ant, *Solenopsis invicta* (Hymenoptera: Formicidae), in China. — *Insects* **12**: 874, 16 pp.

Stark S., Eskelinen A. & Männistö M.K. 2012: Regulation of microbial community composition and activity by soil nutrient availability, soil pH, and herbivory in the tundra. — *Ecosystems* **15**: 18–33.

Steele C., King J., Boughton E. & Jenkins D. 2020: Distribution of the red imported fire ant *Solenopsis invicta* (Hymenoptera: Formicidae) in Central Florida pastures. — *Environ. Entomol.* **49**: 956–962.

Su J., Liu W., Hu F., Miao P., Xing L. & Hua Y. 2023: The distribution pattern and species richness of scorpionflies (Mecoptera: Panorpidae). — *Insects* **14**: 332, 20 pp.

Sung S., Kwon Y.S., Lee D.K. & Cho Y. 2018: Predicting the potential distribution of an invasive species, *Solenopsis invicta* Buren (Hymenoptera: Formicidae), under climate change using species distribution models. — *Entomol. Res.* **48**: 505–513.

Sutherst R.W. & Maywald G. 2005: A climate model of the red imported fire ant, *Solenopsis invicta* Buren (Hymenoptera: Formicidae): implications for invasion of new regions, particularly Oceania. — *Environ. Entomol.* **34**: 317–335.

Tang X., Deng Y., He Z., Zhou M., Yuan Y. & Zeng K. 2025: Modelling the potential distribution and niche shift of *Solenopsis invicta* Buren under climate change and invasion process. — *Front. Forests Global Change* **8**: 1659630, 18 pp.

Travanty N.V. 2021: *Structure of the Bacterial Communities of the American Dog Tick, the Red Imported Fire Ant and Ant Nest Soil, and Behavioral Responses of the Red Imported Fire Ant to Bacterial Isolates.* PhD Thesis, North Carolina State University, 24 pp.

Veloz S.D. 2009: Spatially autocorrelated sampling falsely inflates measures of accuracy for presence-only niche models. — *J. Biogeogr.* **36**: 2290–2299.

Vinson S.B. 1997: Invasion of the red imported fire ant (Hymenoptera: Formicidae): spread, biology, and impact. — *Am. Entomol.* **43**: 23–39.

Vogt J.T., Wallet B. & Freeland T.B. 2008: Imported fire ant (Hymenoptera: Formicidae) mound shape characteristics along a north-south gradient. — *Environ. Entomol.* **37**: 198–205.

Wang L. & Lu Y. 2017: Red imported fire ant *Solenopsis invicta* Buren. In Wan F., Jiang M. & Zhan A. (eds): *Biological Invasions and Its Management in China, Vol. 1.* Springer, Dordrecht, pp. 299–315.

Wang H., Zhang Q., Liu R., Sun Y., Xiao J., Gao L., Gao X. & Wang H. 2022: Impacts of changing climate on the distribution of *Solenopsis invicta* Buren in Mainland China: Exposed urban population distribution and suitable habitat change. — *Ecol. Indicat.* **139**: 108944, 10 pp.

Wang X., Qin Y., Xu Y., Feng X., Zhao S., Lu Y. & Li Z. 2023: Surveillance and invasive risk of the red imported fire ant, *Solenopsis invicta* Buren in China. — *Pest Manag. Sci.* **79**: 1342–1351.

Ward D. 2009: The potential distribution of the red imported fire ant, *Solenopsis invicta* Buren (Hymenoptera: Formicidae), in New Zealand. — *N. Z. Entomol.* **32**: 67–75.

Warren D.L., Wright A.N., Seifert S.N. & Shaffer H.B. 2014: Incorporating model complexity and spatial sampling bias into ecological niche models of climate change risks faced by 90 California vertebrate species of concern. — *Divers. Distrib.* **20**: 334–343.

Wei T., Simko V., Levy M., Xie Y., Jin Y. & Zemla J. 2017: *Package 'Corrplot.' Statistician.* URL https://github.com/taiyun/corrplot.

Wickham H., Chang W. & Wickham M.H. 2016: *Package 'ggplot2'. Create Elegant Data Visualisations Using the Grammar of Graphics. Version 2*. URL: https://ggplot2.tidyverse.org.

Wojcik D.P. 1983: Comparison of the ecology of red imported fire ants in North and South America. — *Fla Entomol.* **66**: 101–111.

Wolters V. 2000: Invertebrate control of soil organic matter stability. — *Biology Fertility Soils* **31**: 1–19.

Xi Y., Lu Y., Zeng L. & Liang G. 2010: Influence of *Solenopsis invicta* Buren on the physical and chemical properties of soils in litchi orchards. — *J. Environ. Entomol.* **32**: 145–151.

Xu Y., Zeng L., Lu Y. & Liang G. 2009: Effect of soil humidity on the survival of *Solenopsis invicta* Buren workers. — *Insectes Soc.* **56**: 367–373.

Zeng L., Lu Y., He X., Zhang W. & Liang G. 2005: Identification of red imported fire ant, *Solenopsis invicta*, to invade mainland China and infestation in Wuchuan, Guangdong. — *Chinese Bull. Entomol.* **42**: 144–148.

Zhan P., Wang F., Xia P., Zhao G., Wei M., Wei F. & Han R. 2022: Assessment of suitable cultivation region for *Panax notoginseng* under different climatic conditions using MaxEnt model and high-performance liquid chromatography in China. — *Industrial Crops Products* **176**: 114416, 12 pp.

Zhang R., Li Y., Liu N. & Porter S.D. 2007: An overview of the red imported fire ant (Hymenoptera: Formicidae) in mainland China. — *Fla Entomol.* **90**: 723–731.

Zhang Y., Li S., Li H., Wang R., Zhang K.-Q. & Xu J. 2020: Fungi-nematode interactions: Diversity, ecology, and biocontrol prospects in agriculture. — *J. Fungi* **6**: 206, 24 pp.

Zhao H., Xian X., Zhao Z., Zhang G., Liu W. & Wan F. 2022: Climate change increases the expansion risk of *Helicoverpa zea* in China according to potential geographical distribution estimation. — *Insects* **13**: 79, 17 pp.

Received January 17, 2026; revised and accepted March 17, 2026
Published online April 16, 2026

Online supplementary files:

S1 (http://www.eje.cz/2026/014/S01.xlsx). Table S1. Statistical output of linear and quadratic GLMs modeling species-environment relationships.

S2 (http://www.eje.cz/2026/014/S02.xlsx). Table S2. Correlation analysis of climatic variables used in initial MaxEnt model with *S. invicta* across China.

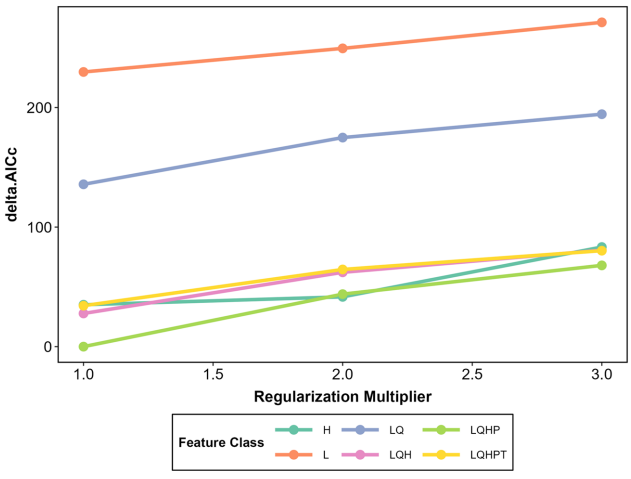

Fig. S1. The delta AICc-value of the model under user-specified range of regularization multiplier (RM) and feature combinations (FCs) for *S. invicta*.

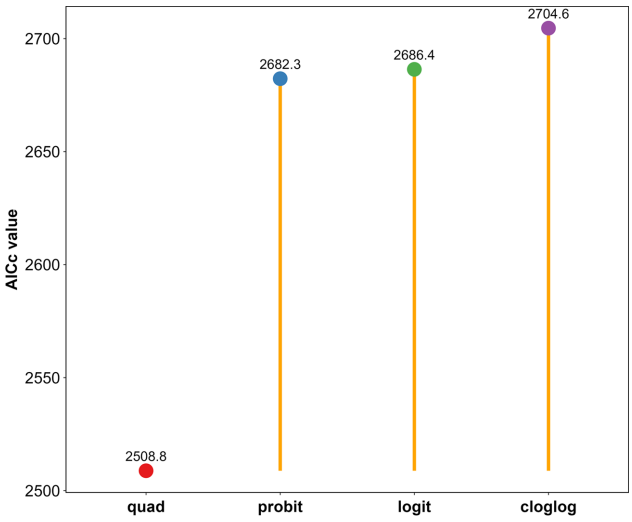

Fig. S2. Comparison of AICc values among GLMs based on 39 predictors influencing *S. invicta* distribution in China.

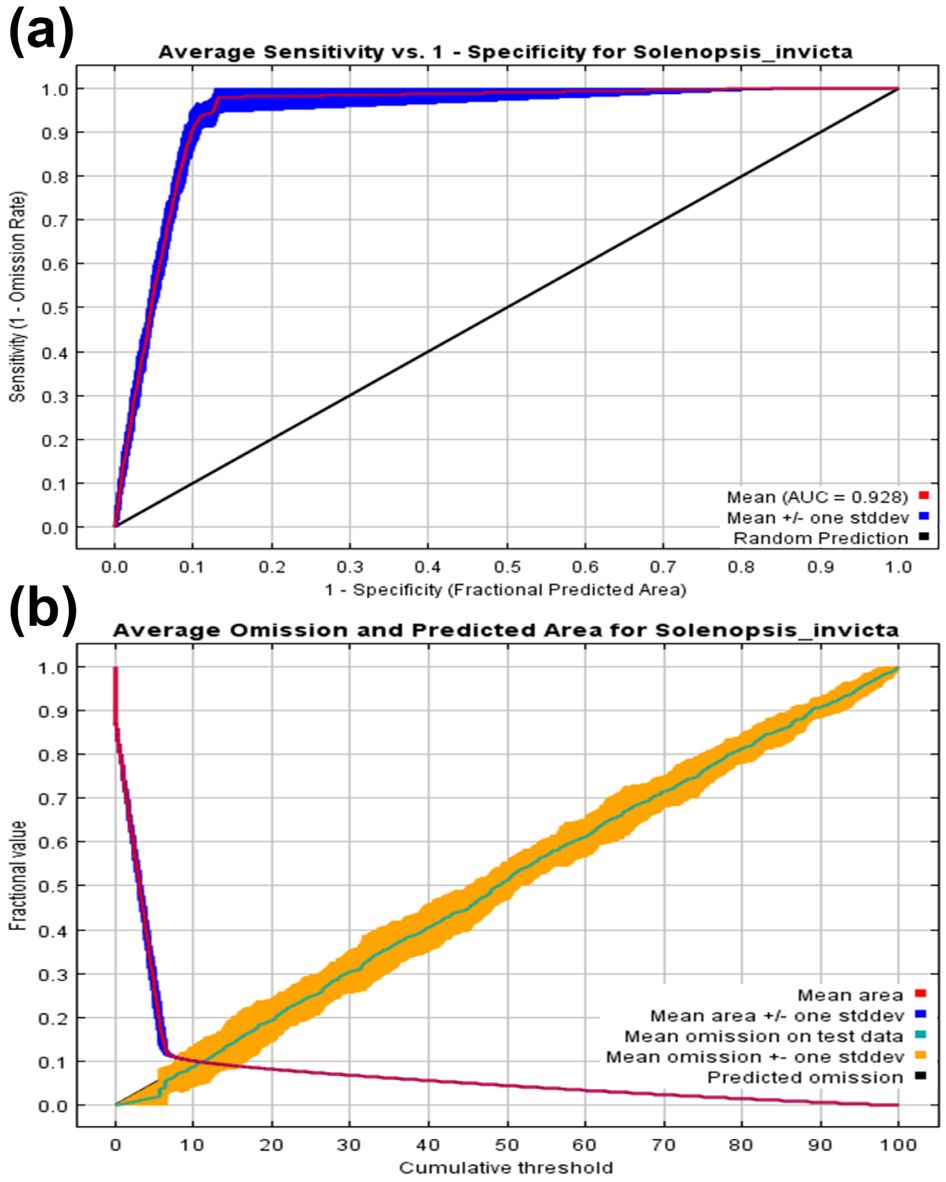

Fig. S3. MaxEnt model results for *S. invicta*: (a) receiver operator characteristic curve (ROC) showing the predictive accuracy of the model; and (b) omission and predicted area curve.